PRAMANA
— journal of
physics

Vol. 52, No. 4
April 1999
pp. 401–408

Lifetimes of nuclear excited states with neutron gated recoil distance method

R PALIT*, P K JOSHI, S NAGARAJ, H V PANCHAL and H C JAIN
Tata Institute of Fundamental Research, Homi Bhabha Road, Mumbai 400 005, India
*Email: palit@tifr.res.in

MS received 11 December 1998

Abstract. A motor driven plunger has been constructed for measuring lifetimes of nuclear excited states in pico second region. An array consisting of six neutron detectors was used to clean up γ-spectra obtained with CS-HPGe detectors. Lifetimes of low excited states in neutron deficient nuclei with low production cross-section e.g. ^{81}Y, ^{77}Kr and ^{78}Rb are reported.

Keywords. Lifetime; recoil distance method; neutron array.

PACS No. 21.10

1. Introduction

The electromagnetic transition probabilities have provided valuable information on intrinsic structure of nuclear excited states [1,2] for a long time. The lifetimes of nuclear excited states produced in heavy ion fusion reactions vary from microseconds to tens of femtoseconds with increasing angular momentum and excitation energies. There are different techniques for measurements depending upon the range of lifetimes. Thus, nanosecond/microsecond beam pulsing is used to measure lifetimes of $\sim 10^{-4}$ to 10^{-9} sec, while lineshape analysis method [3] is used for lifetimes in the region of 10^{-12} to 10^{-14} sec. The recoil distance method (RDM) [4,5,6] is most useful in the intermediate region i.e., from about a picosecond to a few nanoseconds. Since RDM involves measurement of singles γ-ray spectra, the low energy γ-peaks sitting on large background introduce large statistical errors. If the γ-ray of interest belongs to a weak reaction channel, the corresponding γ-peak may be barely visible. Finally, the heavy ion fusion reactions have a large number of reaction channels and the γ-ray of interest may belong to more than one reaction channel. The above difficulties can be addressed through coincidence experiments which will enable selection of reaction channels and reduction of background under the γ-peak. The γ-γ coincidences provide better peak to background ratio and also provide good selection of reaction channel. But it requires high resolution and high efficiency γ-detector array with a large number of detectors. On the other hand, the neutron-gamma coincidences provide an easier and reasonably effective way to clean up the spectra and substantially reduce the

number of reaction channels. An array of six neutron detectors (6″ dia × 5″ thick) covering nearly 1.5π solid angle has been used in coincidence with two CS-HPGe detectors to obtain high (intrinsic) neutron detection efficiency. A new recoil distance set-up allowed a compact geometry both for neutron array and CS-HPGe detector – thereby providing high coincidence efficiency. The measurement of lifetimes of some of the weakly populated levels in ^{81}Y, ^{78}Rb and ^{77}Kr with the neutron gated recoil distance method (NGRDM) mentioned above are reported for the first time in this communication.

2. Experimental details

In the present work, the nuclear excited states in ^{81}Y, ^{78}Rb and ^{77}Kr were populated by bombarding an 115 MeV ^{27}Al beam onto a thin, flat and uniform target of enriched ^{58}Ni. The residual nuclei recoil out of the target and travel in vacuum in a forward cone until they are stopped in a thick, flat and uniform stopper foil placed at a distance d from the target. The target and stopper foils are kept parallel to each other. γ-rays de-exciting the residual nuclei are detected in CS-HPGe detectors placed at angle 'θ' with respect to the beam direction. The γ energy is Doppler shifted if it is emitted in flight, but unshifted (narrow) peak is obtained if γ-ray is emitted after the nucleus has come to rest in the stopper foil. The average velocity $\bar{v}$ of the recoiling ions is determined from the difference between the centroids of the shifted and unshifted γ-peaks through the equation:

$$E_s = E_0(1 + \beta \cos\theta), \tag{1}$$

where E_0 is the unshifted γ-ray energy, E_s the energy of shifted peak, $\beta(= (\bar{v}/c))$ the average recoil velocity and θ the angle of emitted γ-rays with respect to the beam direction. The lifetime τ of the nuclear excited state is derived from a measurement of the relative intensities of the shifted and unshifted γ-peaks as a function of the distance d between the target and stopper. The measurement of small lifetimes requires high recoil velocity and a small value of minimum distance of approach (d_0) between the target and stopper.

A schematic diagram of the plunger is shown in figure 1. The target was prepared from a 500 μgm/cm^2 thick enriched ^{58}Ni foil which was stretched through standard techniques [6,7]. The target holder was mounted on rods with 29 cms length and 4 mm diameter. The rods were made of invar to minimize the thermal expansion effects. The stretched stopper foil ($\sim$10 mg/cm^2 thick tantalum foil) was mounted on a set of other three rods. The parallelism between the target and stopper foils determines the minimum distance of approach between them. It was achieved by adjusting the plane of the stopper foil with the help of springs and screws holding the stopper holder. The target foil was moved with respect to the stopper foil in steps of 1μm (or more) by means of a 'Burleigh inchworm motor'. The motor movement was triggered with the help of a computer which sent instruction to the Burleigh inchworm motor controller (model no. 6000). The relative motion of the target and stopper foils was monitored through a measurement of capacitance [5,6]. The minimum distance of approach was obtained from a plot of C^{-1} vs d and was found to be $\sim$16 μm in the present experiment.

The top view of the complete experimental set-up is also shown in figure 1. The beam was dumped at the end of the vacuum chamber in a thick tantalum sheet. This was surrounded by Pb sheets of thickness $\sim$2 mm, outside the vacuum chamber to absorb γ-rays

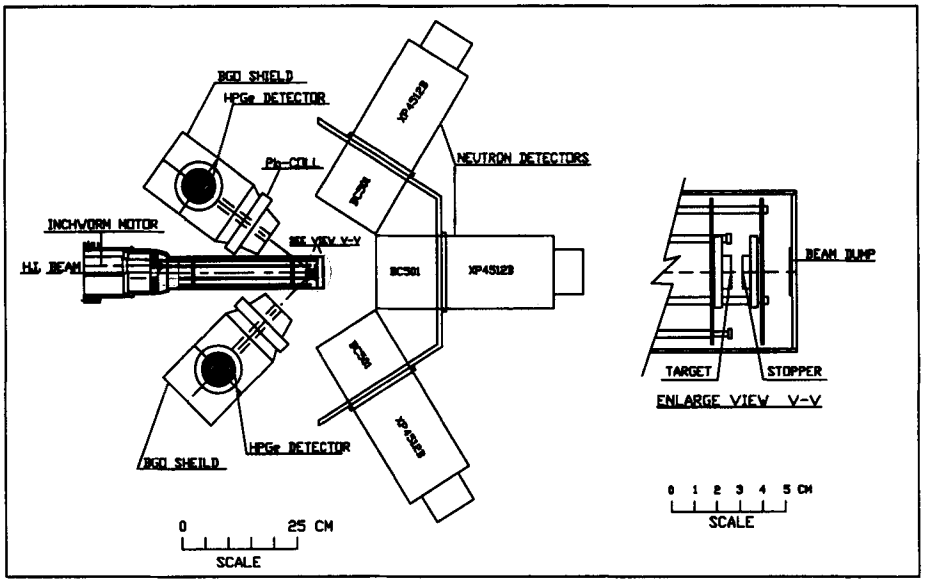

Figure 1. Schematic diagram (top view) of the recoil distance set-up neutron array and CS-HPGe detectors.

emitted by the beam dump. Two CS-HPGe detectors were kept at +144° and −135°, respectively, with respect to the beam direction at a distance of ∼ 25 cms from the target. The neutron array was placed such that the distance of each detector was ∼12 cm from the target. The neutron detectors consist of Bicron BC501 liquid organic scintillator cells mounted on Phillips XP4512B or XP2140 photomultiplier tubes. Standard pulse shape discrimination technique has been used [8] to separate the neutron and gamma peaks in each detector. A typical spectrum showing the separation of neutron and gamma peaks is provided in figure 2 and gives a figure of merit FOM = 1.24. The neutron peaks in each detector were selected by adjusting the lower and upper thresholds in the TAC/SCA. The TTL output was converted to NIM fast signal and applied to the inputs of an Octal constant fraction discriminator. The neutron multiplicity 'M' and 'OR' signals were obtained from the output of the Octal CFD. The master gate was generated with the 'AND' of 'OR' signal from the neutron array and 'OR' of both CS-HPGe detectors. Three parameter-list mode data was collected with energy outputs of two CS-HPGe detectors and neutron multiplicity output as parameters. Singles γ-spectra were also collected simultaneously in a separate data acquisition system. Figure 3 shows a partial γ-ray spectrum (a) singles and (b) neutron gated obtained with 115 MeV ^{27}Al beam incident on 500 μgm/cm^2 thick ^{58}Ni foil. The advantage of neutron gating can be well appreciated in this figure. The 503 keV from ^{78}Rb and 571 keV peak from ^{81}Y are barely visible in singles γ-ray spectrum. But both of them have good peak to background ratios in neutron gated spectrum and enabled us to measure lifetimes belonging to these transitions.

It is seen that the efficiency of the neutron array is ∼ 7% as obtained from the ratio of the areas under the γ peaks in the neutron gated spectrum for one neutron channels and singles γ-ray spectrum. The efficiency for the $2n$ channels is ∼ 16%.

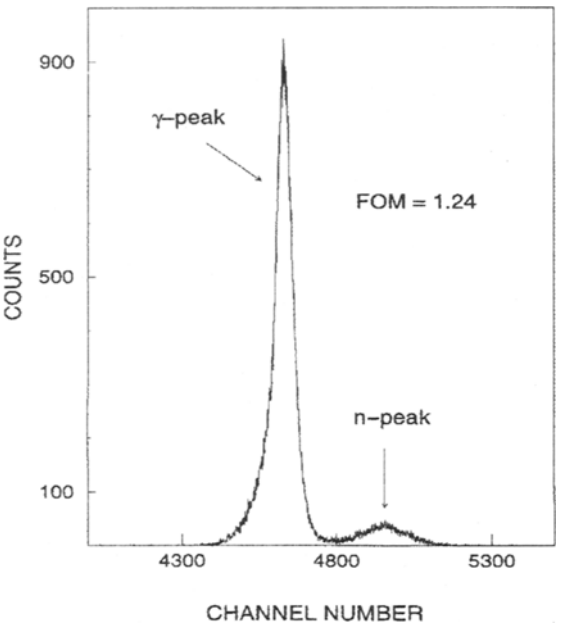

Figure 2. A typical spectrum from one of the neutron detectors showing the neutron and γ peaks after $n - \gamma$ discrimination. The figure of merit FOM = 1.24 was obtained from this detector.

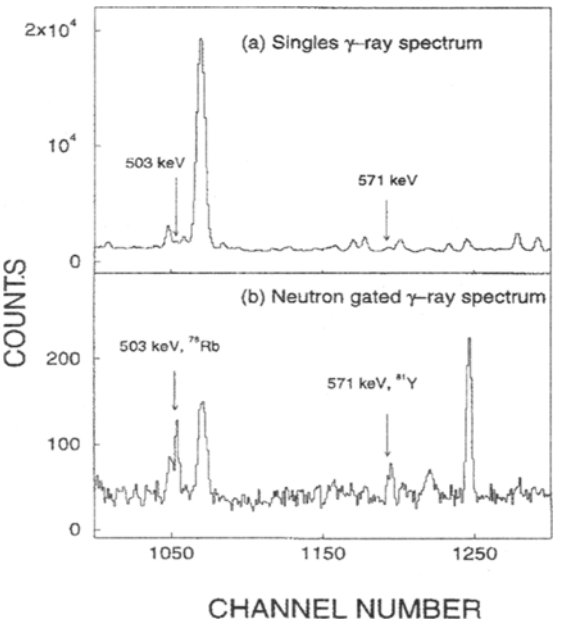

Figure 3. Partial γ-ray spectra (a) Singles and (b) Neutron gated obtained with 115 MeV ^{27}Al beam incident on a 500 μgm/cm^2 thick ^{58}Ni foil.

3. Measurements and results

The measurement of the separation between the centroids of the unshifted and shifted γ peaks in ^{27}Al + ^{58}Ni reaction at 115 MeV ^{27}Al beam energy showed that the average velocity of residual nuclei for most of the reaction channels is $(\bar{v}/c) \sim 0.027 \pm 0.01$. The operation of the plunger set-up was checked through a measurement of known lifetimes of low excited states in ^{78}Kr, ^{80}Sr and ^{81}Y. The γ-spectra were obtained for several target to stopper distances between 16 μm and 1 mm. The intensity of the stopped peak (I_s) is given by

$$I_s = I_0 \exp(-d/\bar{v}\tau) + K, \tag{2}$$

where, I_0 is the intensity of the stopped peak for zero separation, d the distance between target and stopper and K is a constant. If one takes the top feeding time into account, the above equation will be modified to

$$I_s = \frac{A}{\tau_f - \tau}\left[\tau_f \exp\left(-\frac{d}{\tau_f \bar{v}}\right) - \tau \exp\left(-\frac{d}{\tau \bar{v}}\right)\right] + K, \tag{3}$$

where, A and K are constants, τ is the mean lifetime of the state, τ_f is the top feeding time and d is the distance between the target and stopper. The normalized stopped peak intensities as a function of d were fitted with (3) to obtain the mean lifetime of the deexciting level. The measurements gave a value of $\tau(4^+) = 3.93(31)$ ps for the 1119 keV (4^+) state in ^{78}Kr, $\tau(4^+) = 4.10(28)$ ps for the 981 keV (4^+) state in ^{80}Sr and $\tau(13^+/2) = 4.0(7)$ ps for the 840 keV $(13^+/2)$ state in ^{81}Y . These are in good agreement with the values reported in [9–11], respectively. The decay curves i.e., the stopped peak intensity in the CS-HPGe detector kept at -135^o with respect to the beam axis as a function of distance for the 119 keV $(9^+/2) \rightarrow (7^+/2)$ transition in ^{81}Y, 128 keV $(9^+/2) \rightarrow (7^+/2)$ transition in ^{77}Kr, 430 keV $(8^+ \rightarrow 6^+)$ transition in ^{78}Rb [12] and 225 keV $(8^+ \rightarrow 6^+)$ transition are shown in figure 4. The stopped peak intensities in the second CS-HPGe detector vs the distances between the target and stopper were also fitted with (3) to get the mean lifetime of the states. The average values of the lifetimes for excited states in ^{81}Y, ^{77}Kr and ^{78}Rb obtained from the two CS-HPGe detectors are listed in table 1.

4. Discussion

The lifetimes listed in table 1 have been measured for the first time using the new plunger set-up which made it possible to gate the γ-ray spectra with the neutron detector array. The measured lifetimes are used to obtain information on shape and collectivity in ^{81}Y, ^{77}Kr and ^{78}Rb. The $B(M1), B(E2)$ and Q_t values have been obtained from the measured lifetimes using the intensities and branching ratios of γ-transitions from [11–14] and the K-values of the bandheads required for calculations were obtained from the energy level diagram given by W. Nazarewicz *et al* [15]. According to this diagram, the odd proton is most likely to occupy the $\pi[422](5/2)$ orbital leading to $K = (5/2)$ for the positive parity band in ^{81}Y. This is supported by the $(5^+/2)$ spin for the ground state in ^{81}Y [12]. On the other hand, the odd proton and neutron could occupy the $\pi[431](3/2)$ and $\nu[422](5/2)$

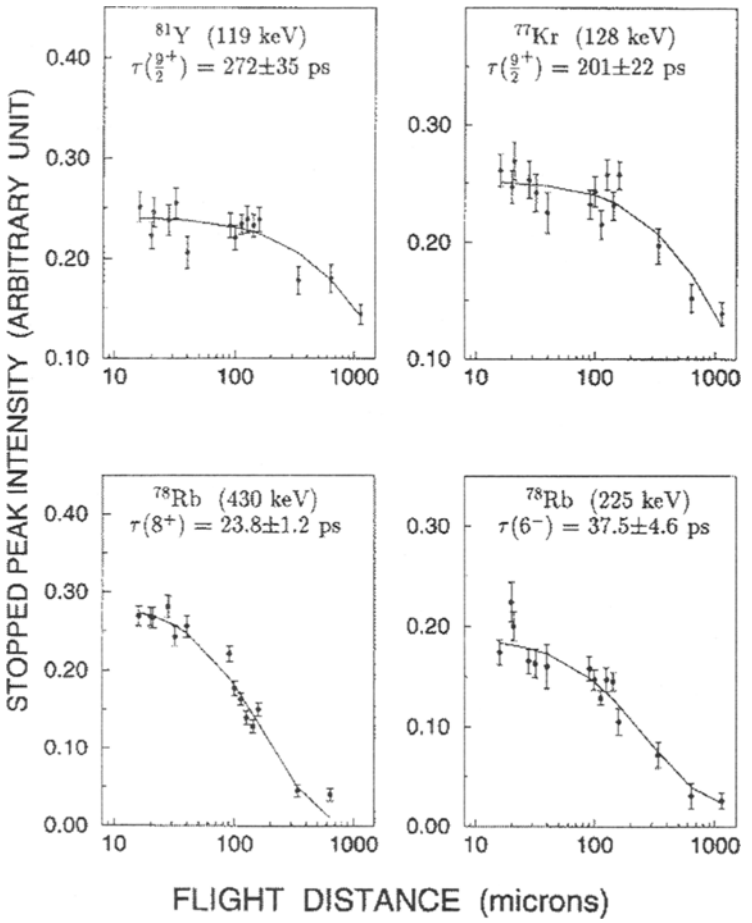

Figure 4. The stopped peak intensity in CS-HPGe detector kept at +135° vs flight distance for 119 keV $(9^+/2 \rightarrow 7^+/2)$ transition in ^{81}Y, 128 keV $(9^+/2 \rightarrow 7^+/2)$ transition in ^{77}Kr, 430 keV transition $(8^+ \rightarrow 6^+)$ in ^{78}Rb and 225 keV $(6^- \rightarrow 5^-)$ transition in ^{78}Rb. The solid curves are fit to the data.

orbitals leading to $K = 4$ for the positive parity band in ^{78}Rb. This is consistent with 4^+ spin for the lowest energy level in the positive parity band [13]. Similarly, the occupation of the $\pi[431](3/2)$ and $\nu[301](3/2)$ orbitals gives $K = 3$ for the negative parity band in ^{78}Rb. The $B(M1)$, $B(E2)$ and Q_t values obtained in the present work are listed in the last two columns in table 1. The large degree of collectivity at low excitation energies is quite evident from lifetime measurements giving $Q_t = 3.16(7)$ eb and $\beta_2 = 0.40(1)$ for the $(9^+/2)$ state and $Q_t = 3.5(3)$ eb corresponding to $\beta_2 = 0.43(3)$ for the $(13^+/2)$ state in ^{81}Y. TRS calculations for ^{81}Y reported in [12] show that the deformation in the yrast band with parity $\pi = +$ and signature $\alpha = +(1/2)$ is quite stable up to $\hbar\omega = 0.294$ MeV with $\beta_2 = 0.37$ and $\gamma \sim 0^o$ leading to a value of $Q_t = 3.65$ eb in agreement with the experimentally observed value in the present work. The present measurement gave a value of $Q_t = 2.2(2)$ eb leading to $\beta_2 = 0.31(3)$ for the $(9^+/2)$ state in ^{77}Kr. This is in good agreement with the

Table 1. Lifetimes of nuclear excited states in ^{81}Y, ^{77}Kr and ^{78}Rb.

Nucleus	Level (keV)	$I_i \rightarrow I_f$ $\hbar$	Transition Energy (keV)	Lifetime ps	$B(E2)$ or $B(M1)$ e^2fm^4 or μ_n^2	Q_t (Expt.) eb
^{81}Y	269.0	$9/2^+ \rightarrow 7/2^+$	119.0	249(11)*	0.09(1)‡	
		$9/2^+ \rightarrow 5/2^+$	269.0		995(45)	3.16(7)[a]
^{81}Y	840.0	$13/2^+ \rightarrow 9/2^+$	571.0	4.0(7)	2614(458)	3.5(3)[a]
^{77}Kr	279.0	$9/2^+ \rightarrow 7/2^+$	129.0	222(42)*	0.104(21)‡	
		$9/2^+ \rightarrow 5/2^+$	279.0		474^{+111}_{-75}	2.2(2)[a]
^{78}Rb	422.8	$6^+ \rightarrow 4^+$	308.0	101(11)*	672(75)	3.2(2)[b]
^{78}Rb	667.3	$7^+ \rightarrow 6^+$	244.0	17.6(3.0)*	0.20(3)‡	
		$7^+ \rightarrow 5^+$	397.0		562^{+164}_{-82}	$2.2^{+0.3}_{-0.2}$[b]
^{78}Rb	852.9	$8^+ \rightarrow 6^+$	430.0	24(1)*	1468(62)	3.0(1)[b]
^{78}Rb	488.8	$6^- \rightarrow 5^-$	225.0	34(3)*	0.083(8)‡	
		$6^- \rightarrow 4^-$	378.0		1295(115)	2.94(14)[c]
^{78}Rb	767.1	$7^- \rightarrow 5^-$	503.0	7.1(1.0)*	2264^{+410}_{-253}	$3.4^{+0.3}_{-0.2}$[c]

*__New lifetimes__; weighted average of two detectors at + 144° and − 135°.
‡Multipolarity: $M1 + E2$. Pure $M1$ assumed to calculate $B(M1)$.
[a] Assuming K=2.5, [b] Assuming K=4, [c] Assuming K=3

theoretical value of $\beta_2 = 0.34$ for the $K^\pi = (5^+/2)$ bandhead in [15]. The TRS calculations for ^{78}Rb presented in [13] predict a nearly prolate configuration with $\beta_2 = 0.34$ and $\gamma \sim 0°$ for both the positive and negative parity bands at low excitation energies. The theoretical Q_t values at low frequencies [13] both for the positive and negative parity states match quite well with the experimental Q_t values obtained in the present work except for the experimental Q_t value for the $7^+ \rightarrow 5^+$ transition which is somewhat lower compared to other values obtained in ^{78}Rb. As mentioned above, $K = 3$ has been used for the negative parity states in the present calculations. This is further justified by the observation that $K = 4$ gives unrealistically high values of β_2 both for the 6^- and 7^- states in ^{78}Rb.

In summary, the new plunger set-up in conjunction with the neutron array has enabled us to measure lifetimes of low lying nuclear excited states which could not be obtained from the singles measurements. The results of the present measurements are in agreement with the theoretical prediction of large prolate deformation and shell gap in the vicinity of $Z = 38$ nuclei in mass ~80 region.

Acknowledgements

Authors would like to thank the TIFR pelletron staff for the smooth functioning of the accelerator during the experiment and the staff of the central workshop for the fabrication of the mechanical parts of the plunger set-up and the neutron detector array. Authors would like to thank Pratik Majumdar for his participation in this experiment.

References

[1] P J Twin, A H Nelson, B M Nyako, D Howe, H W Cranmer-Gordon, D Elenkov, P D Forsyth, J K Jabber, J F Sharpey-Schafer, *Phys. Rev. Lett.* **55**, 1380 (1985)

[2] S D Paul, H C Jain, S Chattopadhyay, J A Sheikh, M L Jhingan, *Phys. Rev.* **C51**, 2959 (1995)

[3] L G Elliot and R E Bell, *Phys. Rev.* **74**, 1869 (1948)

[4] T K Alexander and K W Allen, *Can. J. Phys.* **43**, 1563 (1965)

[5] T K Alexander and A Bell, *Nucl. Instrum. Methods* **81**, 22 (1970)

[6] H C Jain, S Chattopadhyay, Y K Agrawal, M L Jhingan, S K Mitra, H V Panchal and Amit Roy, *Pramana-J. Phys.* **37**, 269 (1991)

[7] J L Gallant, *Nucl. Instrum. Methods* **81**, 27 (1970)

[8] J Toke, S A Masserant, S P Baldwin, B Lott, W U Schroder and X Zhao, *Nucl. Instrum. Methods* **A334**, 653 (1993)

[9] H P Hellmeister, J Keinonen, K P Lieb, U Kaup, R Rascher, R Ballini, J Delaunay and H Dumont, *Nucl. Phys.* **A332**, 241 (1979)

[10] C J Lister, B J Varley, H G Price and J W Olness, *Phys. Rev. Lett.* **49**, 308 (1982)

[11] P K Joshi, S D Paul, S Nagaraja and H C Jain, *DAE symposium on nuclear physics* (1996)

[12] T D Johnson, A Raguse, C J Gross, M K Kabadiyski, K P Leib, D Rudoplh, M Weiszflog, T Burkardt, J Eberth, S Skoda, *Z. Phys.* **A350**, 189 (1994)

[13] A Kaye, J Doring, J W Holcomb, G D Johns, T D Johnson, M A Riley, G N Sylvan, P C Womble, V A Wood, S L Tabor and J X Saladin, *Phys. Rev.* **C54**, 1038 (1996)

[14] G N Sylvan, G Doring, G D Johns, S L Tabor, C J Gross, C Baktash, H Q Jin, D W Stracener, P F Hua, M Korolija, D R LaFosse, D G Sarantites, F Cristancho, E Landulfo, J X Saladin, B Cederwall, I Y Lee, A O Macchiavelli, W Rathbun and A Vander Molen, *Phys. Rev.* **C56**, 772 (1997)

[15] W Nazarewicz, J Dudek, R Bengtsson, T Bengtsson and I Ragnarsson, *Nucl. Phys.* **A435**, 397 (1985)